© 2016. This manuscript version is made available under the CC-BY-NC-ND 4.0 license
http://creativecommons.org/licenses/by-nc-nd/4.0/

A framework for radial data comparison and its application to fingerprint analysis

C. Marco-Detchart[a], J. Cerron[a], L. De Miguel[a,b], C. Lopez-Molina[a,c], H. Bustince[a,b], M. Galar[a,b]

[a]*Dpto. de Automatica y Computacion, Universidad Publica de Navarra, Campus Arrosadia s/n, 31006 Pamplona, Spain*
[b]*Institute of Smart Cities, Universidad Publica de Navarra, Campus Arrosadia s/n, 31006 Pamplona, Spain*
[c]*KERMIT, Dept. of Mathematical Modelling, Statistics and Bioinformatics, Ghent University, Coupure links 653, 9000 Gent, Belgium*

Abstract

This work tackles the comparison of radial data, and proposes comparison measures that are further applied to fingerprint analysis. First, we study the similarity of scalar and non-scalar radial data, elaborated on previous works in fuzzy set theory. This study leads to the concepts of Restricted Radial Equivalence Function and Radial Similarity Measure, which model the perceived similarity between scalar and vectorial pieces of radial data, respectively. Second, the utility of these functions is tested in the context of fingerprint analysis, and more specifically, in the singular point detection. With this aim, a novel template-based singular point detection method is proposed, which takes advantage of these functions. Finally, their suitability is tested in different fingerprint databases. Different similarity measures are considered to show the flexibility offered by these measures and the behavior of the new method is compared with well-known singular point detection methods.

Keywords: Radial data, Restricted equivalence function, similarity measure, fingerprint singular point detection

1. Introduction

The ability to quantify the similarity between two objects in a given universe is a pillar in applied fields of research. Historically, this quantification has been based on metrics, which are able to capture, in a sensible (and coherent) manner, the proximity of any two objects in a measurable universe. Metrics hold very interesting properties, specifically triangular inequality, which preserves the notion that the shortest path between two objects is the straight one. However, they also impose the need for the representation of the objects in a metric space, as well as notions (e.g. transitivity), which are not natural in certain scenarios [1].

When it comes to measuring dissimilarity between multivalued data, L_p metrics often come as a straightforward option; the most relevant case is $p = 2$, which recovers the Euclidean metric. The L_p metric has been long criticized, specially regarding its low accuracy in capturing perceptual dissimilarities. For example, Attneave stated that the assumption that the *psychological space is Euclidean in its character* is *exceedingly precarious* [2]. Obviously, there exist other metrics yielding more (perceptually) accurate measurements of dissimilarity, specially when they are designed for well-defined scenarios [3, 4]. The debate about the restrictivity of the requisites imposed by metrics is still open [5]. Literature contains both practical [6], and theoretical criticisms. Authors as Tversky [7] or Santini and Jain [5] criticized the necessity of imposing metric conditions to similarity measures, as well as the representation of objects in metric spaces, given that they are often missing in human understanding. Tversky [7, 8] also revisited the necessity of symmetry and the directional nature of comparisons in certain scenarios. Finally, the low representativity of the values given by metrics for large-range comparisons has also been under debate [9, 10].

Different mathematical theories have tackled the modelling of similarity with tools other than metrics, leading to what Zadeh referred to as *a vast armamentarium* of techniques for comparison [11]. In fact, even axiomatic

Email addresses: cedric.marco@unavarra.es (C. Marco-Detchart), juan.cerron@unavarra.es (J. Cerron), laura.demiguel@unavarra.es (L. De Miguel), carlos.lopez@unavarra.es (C. Lopez-Molina), bustince@unavarra.es (H. Bustince), mikel.galar@unavarra.es (M. Galar)

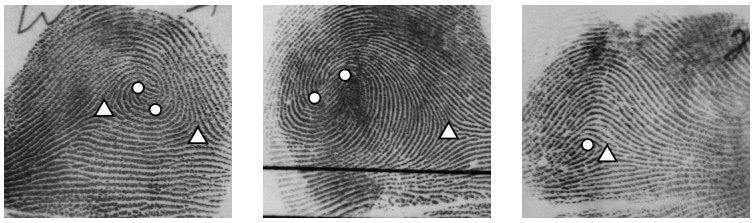

Figure 1: Examples of singular points detected on fingerprints extracted from the NIST-4 dataset [19]. The *deltas*, represented as triangles, are triangular-like ridge confluences, while *cores*, represented as circles, take place at curly ridge structures.

representations of non-metric comparison frameworks have appeared in the literature (e.g. [7] for set-based similarity, or [12, 13] for T-indistinguishability). In the context of fuzzy set theory, a range of authors have elaborated on the semantic interpretation of similarities and dissimilarities [5], since Zadeh introduced similarity as an extension of equivalence [11]. This is natural, considering that the concepts of proximity and similarity (as well as ordering or clustering) are strongly related to human interpretation, and hence prone to be tackled in fuzzy terms. A large variety of proposals have appeared for modelling both similarity and dissimilarity; in this work we focus our interest on two of them: Restricted Equivalence Functions (REFs) for the comparison of membership degrees and Similarity Measures (SMs) for the comparison of fuzzy sets on discrete universes [14].

In this paper we propose a definition of the concept of REFs and SMs for radial data. This study is motivated by the increasing relevance of radial data in real applications, especially in those demanding the extraction of information by means of computer vision techniques. Very often, computer vision handles radial data in different flavours (e.g., angular, vector or tensorial data [15]) and consequently demands well-defined operators for different tasks, including data comparison. Typically, the study of radial data has been restricted to radial statistics, which mostly study the fitting and analysis of well-known distributions on radial set-ups. To the best of our knowledge, there are no studies on the quantification of the similarity of elements in a radial universe. This situation has led many researchers to use *ad-hoc* operators to deal with the special conditions of the data, instead of creating a framework in which different operators can be encompassed. For this reason in this work we develop a framework aiming at easing the comparison of radial data. More specifically, we define Restricted Radial Equivalence Functions (RREFs), as well as Restricted Similarity Measures (RSMs), which attempt to mimic the behaviour of REFs and SMs in radial universes.

As a case of study, we present an application of RREFs and RSMs to biometric identification, specifically to singular point detection in fingerprint recognition [16]. Fingerprints can be seen as a set of ridges (lines) that represent the relief of the skin in the fingertip surface. Hence, their analysis is often based on studying the line patterns in a local or semi-local basis. Within fingerprint analysis, a fundamental operation is the detection and localization of the so-called *Singular Points* (SPs), which are structural singularities in the ridges (see Fig. 1). SP detection is often related to specific occurrences in the orientation of the ridges of neighbouring regions, which are usually found using semi-local analysis [17] or complex convolution filters [18].

On this account, a simple yet effective framework for SP detection is presented in this paper by means of RREFs and RSMs, which shows the usefulness and flexibility of these new measures. Furthermore, other well-known SP detection algorithms have been used as a baseline for performance evaluation [20, 21]. In this comparative analysis we have considered two different types of databases: NIST-4 database [19], the most commonly used fingerprint database and synthetic fingerprint databases generated by SFinGe[1].

The remainder of the work is as follows. In Section 2 we review the concepts of REF and SM, as well as some standard notation on radial data. Section 3 is devoted to introduce the concepts of RREF and RSM. Both RREF and RSM are used in Section 4, in which we present our proposal for SP detection in fingerprints. Section 5 includes an experimental study in which we illustrate the performance of our SP detection method, compared to other well-known methods in the literature. Finally, Section 6 gathers some conclusions and a brief discussion on potential future evolutions of our method.

[1] Synthetic Fingerprint Generator: `http://biolab.csr.unibo.it/sfinge.html`

2. Preliminaries

Among the areas in which fuzzy set theory has played a relevant role, data similarity modelling is one of the most prominent. The reason is that the natural concepts of similarity, closeness or likeliness are inherently bounded to human interpretation. Hence, different proposals have appeared to effectively model the comparison of pieces of information. Among these, we find fuzzy metric spaces [6], with interesting advantages over classical metric spaces in terms of interpretability [22] or equivalence and similarity measures [14], which we take as inspiration to develop measures that can handle radial data. Next, we recall the concepts of REF and SM.

Definition 1. *A continuous, strictly decreasing function $n : [0,1] \to [0,1]$ such that $n(0) = 1$, $n(1) = 0$ and $n(n(x)) = x$ for all $x \in [0,1]$ (involutive property) is called strong negation.*

Definition 2. *[14] A mapping $r : [0,1]^2 \to [0,1]$ is said to be a Restricted Equivalence Function (REF) associated with the strong negation n if it satisfies the following:*

(R1) $r(x,y) = r(y,x)$ *for all* $x, y \in [0,1]$*;*

(R2) $r(x,y) = 1$ *if and only if* $x = y$*;*

(R3) $r(x,y) = 0$ *if and only if* $\{x,y\} = \{0,1\}$*;*

(R4) $r(x,y) = r(n(x), n(y))$ *for all* $x, y \in [0,1]$*;*

(R5) For all $x, y, z, t \in [0,1]$*, such that* $x \leq y \leq z \leq t$ *then* $r(y,z) \geq r(x,t)$.

Note that (R5) means that, for all $x, y, z \in [0,1]$, if $x \leq y \leq z$ then $r(x,y) \geq r(x,z)$ and $r(y,z) \geq r(x,z)$.

REFs attempt to capture the perceived similarity between two values in $[0,1]$, which in fuzzy set theory usually represent membership degrees. It is usual to construct REFs from a pair of automorphisms of the unit interval, as proposed in [14], although alternative methods have also been studied [23].

Definition 3. *A continuous, strictly increasing function $\varphi : [a,b] \to [a,b]$ such that $\varphi(a) = a$ and $\varphi(b) = b$ is called automorphism of the interval $[a,b] \subset \mathbb{R}$.*

Proposition 1. *[14] Let φ_1, φ_2 be two automorphisms of the interval $[0,1]$. Then*

$$r(x,y) = \varphi_1^{-1}(1 - |\varphi_2(x) - \varphi_2(y)|)$$

is a REF associated with the strong negation $n(x) = \varphi_2^{-1}(1 - \varphi_2(x))$.

Example. Let $\varphi_1(x) = x$ and $\varphi_2(x) = \sqrt{x}$, then

$$r(x,y) = 1 - |\sqrt{x} - \sqrt{y}| \tag{1}$$

is a REF associated with $n(x) = (1 - \sqrt{x})^2$.

Figure 2 contains the visual representation of several REFs constructed following Prop. 1. Note that in this work we are referring to REFs in the original sense, although the concept has been exported to, e.g. interval data [24]. While REFs are useful to compare scalar data (membership degrees), similarity measures were developed to compare non-scalar data. Even though the measures were initially designed to compare fuzzy sets on discrete universes, they can be further applied to many other objects (e.g. vectors or matrices). Similarity measures were originally proposed by Liu [25] and its definition is trivially applied to $[0,1]^k$.

Definition 4. *[25] A mapping $s : [0,1]^k \times [0,1]^k \to \mathbb{R}^+$ is called k-ary Similarity Measure (SM) associated with the strong negation n if it satisfies the following:*

(S1) $s(\boldsymbol{x}, \boldsymbol{y}) = s(\boldsymbol{y}, \boldsymbol{x})$ *for all* $\boldsymbol{x}, \boldsymbol{y} \in [0,1]^k$*;*

(S2) $s(\boldsymbol{x}, n(\boldsymbol{x})) = 0$ *if and only if* $x_i \in \{0,1\}$ *for all* $i \in \{1, \ldots, k\}$ *and* $n(\boldsymbol{x}) = (n(x_1), \ldots, n(x_k))$*;*

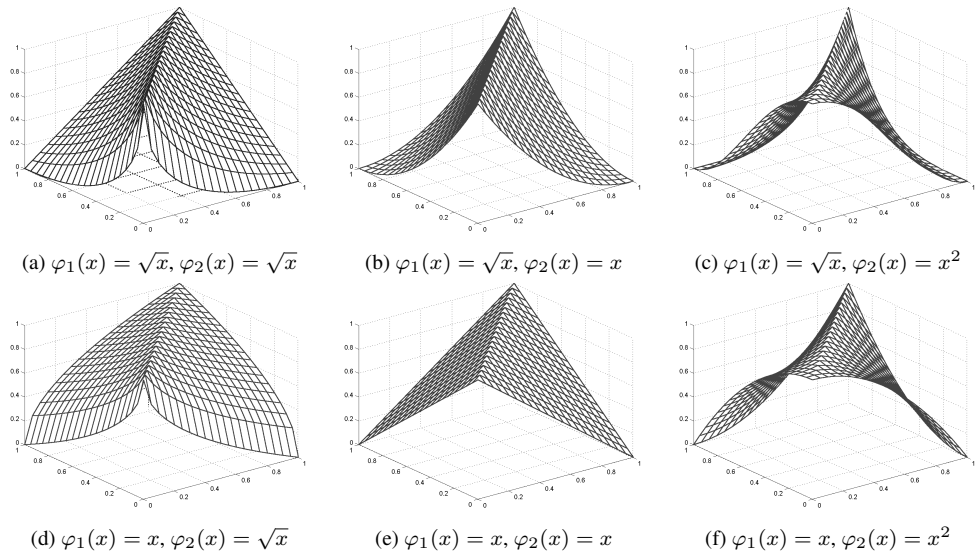

(a) $\varphi_1(x) = \sqrt{x}, \varphi_2(x) = \sqrt{x}$ (b) $\varphi_1(x) = \sqrt{x}, \varphi_2(x) = x$ (c) $\varphi_1(x) = \sqrt{x}, \varphi_2(x) = x^2$

(d) $\varphi_1(x) = x, \varphi_2(x) = \sqrt{x}$ (e) $\varphi_1(x) = x, \varphi_2(x) = x$ (f) $\varphi_1(x) = x, \varphi_2(x) = x^2$

Figure 2: Restricted Equivalence Functions (REFs) created from automorphisms in the unit interval as in Proposition 1.

(S3) $s(\boldsymbol{z},\boldsymbol{z}) = \max_{(\boldsymbol{x},\boldsymbol{y}\in[0,1]^k)} s(\boldsymbol{x},\boldsymbol{y})$ *for all* $z \in [0,1]^k$*;*

(S4) For all $\boldsymbol{x},\boldsymbol{y},\boldsymbol{z},\boldsymbol{t} \in [0,1]^k$*, if* $\boldsymbol{x} \leq \boldsymbol{y} \leq \boldsymbol{z} \leq \boldsymbol{t}$ *then* $s(\boldsymbol{y},\boldsymbol{z}) \geq s(\boldsymbol{x},\boldsymbol{t})$ *where* $\boldsymbol{x} \leq \boldsymbol{y}$ *implies that* $x_i \leq y_i$ *for all* $i \in \{1,\ldots,k\}$.

Similarly to what happens for REFs, the property (S4) is equivalent to: For all $\mathbf{x},\mathbf{y},\mathbf{z} \in [0,1]^k$, if $\mathbf{x} \leq \mathbf{y} \leq \mathbf{z}$ then $s(\mathbf{x},\mathbf{y}) \geq s(\mathbf{x},\mathbf{z})$ and $s(\mathbf{y},\mathbf{z}) \geq s(\mathbf{x},\mathbf{z})$.

Similarity Measures (SMs) can be constructed in different ways, although the most popular method originates from the combination of REFs and aggregation functions [26].

Definition 5. *A mapping* $f : [0,1]^k \to [0,1]$ *is called* k*-ary aggregation operator if it satisfies the following:*

(AO1) If $x_i = 0$ *for all* $i \in \{1,\ldots,k\}$*, then* $f(\mathbf{x}) = 0$*;*

(AO2) If $x_i = 1$ *for all* $i \in \{1,\ldots,k\}$*, then* $f(\mathbf{x}) = 1$*;*

(AO3) f *is increasing in all of its arguments.*

Proposition 2. *[14] Let* r *be a REF and let* f *be a* k*-ary aggregation function such that* $f(\boldsymbol{x}) = 0$ *if and only if* $x_i = 0$ *for all* $i \in \{1,\ldots,k\}$ *and* $f(\boldsymbol{x}) = 1$ *if and only if* $x_i = 1$ *for all* $i \in \{1,\ldots,k\}$*. The function* $s_{[f,r]} : [0,1]^k \times [0,1]^k \mapsto [0,1]$*, given by*

$$s_{[f,r]}(\boldsymbol{x},\boldsymbol{y}) = f(r(x_1,y_1),\ldots,r(x_k,y_k)) \tag{2}$$

is a k*-ary similarity measure which satisfies the following:*

- $s_{[f,r]}(\boldsymbol{x},\boldsymbol{y}) = s_{[f,r]}(\boldsymbol{y},\boldsymbol{x})$ *for all* $\boldsymbol{x},\boldsymbol{y} \in [0,1]^k$*;*
- $s_{[f,r]}(\boldsymbol{x},n(\boldsymbol{x})) = 0$ *if and only if* $x_i \in \{0,1\}$ *for all* $i \in \{1,\ldots,k\}$ *and* $n(\boldsymbol{x}) = (n(x_1),\ldots,n(x_k))$*;*
- $s_{[f,r]}(\boldsymbol{x},\boldsymbol{y}) = 1$ *if and only if* $x_i = y_i$ *for all* $i \in \{1,\ldots,k\}$*;*
- *For all* $\boldsymbol{x},\boldsymbol{y},\boldsymbol{z},\boldsymbol{t} \in [0,1]^k$*, if* $\boldsymbol{x} \leq \boldsymbol{y} \leq \boldsymbol{z} \leq \boldsymbol{t}$ *then* $s_{[f,r]}(\boldsymbol{y},\boldsymbol{z}) \geq s_{[f,r]}(\boldsymbol{x},\boldsymbol{t})$ *where* $\boldsymbol{x} \leq \boldsymbol{y}$ *implies that* $x_i \leq y_i$ *for all* $i \in \{1,\ldots,k\}$*;*
- $s_{[f,r]}(\boldsymbol{x},\boldsymbol{y}) = s_{[f,r]}(n(\boldsymbol{x}),n(\boldsymbol{y}))$ *for all* $\boldsymbol{x},\boldsymbol{y} \in [0,1]^k$.

Next, we include some conventions on the use of radial data that will hold in the remainder of this work. In order to face those cases in which two angles represent the same direction (e.g. $\frac{\pi}{2}$ and $\frac{5\pi}{2}$), an equivalence relation R is defined.

Let $a, b \in \mathbb{R}$. We say that aRb if and only if $a = b + 2k\pi$, where $k \in \mathbb{Z}$. In this way, the equivalence class $[a] = \{b \mid bRa\}$ is the set containing all the data associated with the same direction. In the same way, any semiopen interval whose width is 2π (i.e., an interval of the form $[\omega, \omega+2\pi[$) is the quotient set (a set which contains one element and only one of each equivalence class). In particular, the intervals $[0, 2\pi[$ and $[-\pi, \pi[$ are the most frequently used quotient sets in radial data.

In this work we consider the quotient set $\Omega = [0, 2\pi[$ and we define on Ω the classical operations sum ($\oplus$) and difference ($\ominus$), given by $a \oplus b = [a + b]$ and $a \ominus b = [a - b]$ where $[t]$ denotes the only element $z \in \Omega$ such that zRt. Under these conditions, we refer to *mirroring* as the mapping: $m : \Omega \longrightarrow \Omega$ such that $m(a) = a \oplus \pi$.

In order to properly explain our incoming proposal on the quotient set Ω, we present the general definition of metric.

Definition 6. *A function $d : U \to \mathbb{R}^+$ is called metric on U if it satisfies the following:*

(D1) $d(a, b) = 0$ *if and only if* $a = b$*;*

(D2) $d(a, b) = d(b, a)$ *for all* $a, b \in U$*;*

(D3) $d(a, c) \leq d(a, b) + d(b, c)$ *for all* $a, b, c \in U$.

3. Comparison of radial data

As reported by Fisher [27], radial data has been a subject of analysis since mid-18^{th} century. However, most of the literature on radial data is based on adapting the usage of distributions to the circular set-up, probably because data analysis for natural sciences was the field in which radial data was first studied [28, 29].

One of the open problems in radial data is data comparison. In fact, to the best of our knowledge, no explicit mention to the quantification of similarity between two angles has been performed in the literature. There have been concepts such as the *sample median direction* [27] or the *sample modal direction* [30], and metrics such as the angular metric on $[0, 2\pi[$ ($d^*(a, b) = \min(|b - a|, 2\pi - |b - a|)$), which represents the amplitude of the shortest arc encompassing two angles. However, no development has been made on interpretable measures able to adapt to human perception or evaluation. This section is devoted to develop functions that are able to measure the perceived similarity between scalar and vector angular data. Section 3.1 covers the comparison of scalar radial data, whereas Section 3.2 covers the comparison of vector radial data[2].

3.1. Restricted Radial Equivalence Functions

The comparison of linear data has produced a vast amount of literature, despite coming from a relatively simple concept. The concept of similarity becomes much more intricate when applied to radial data. In this section we define operators that model the comparison of elements in a radial context Ω, all inspired by the operators in Section 2.

Definition 7. *A mapping $r_\theta : \Omega^2 \to [0, 1]$ is called a Restricted Radial Equivalence Function (RREF) associated with the metric d if it satisfies the following:*

(RR1) $r_\theta(a, b) = r_\theta(b, a)$ *for all* $a, b \in \Omega$*;*

(RR2) $r_\theta(a, b) = 1$ *if and only if* $d(a, b) = 0$*;*

(RR3) $r_\theta(a, b) = 0$ *if and only if* $d(a, b)$ *is maximum;*

(RR4) $r_\theta(a, b) = r_\theta(m(a), m(b))$ *for all* $a, b \in \Omega$*;*

[2]There exist in the literature certain controversy w.r.t. the most adequate name of radial data, including angular data or radial data. In this manuscript we adhere to *radial*.

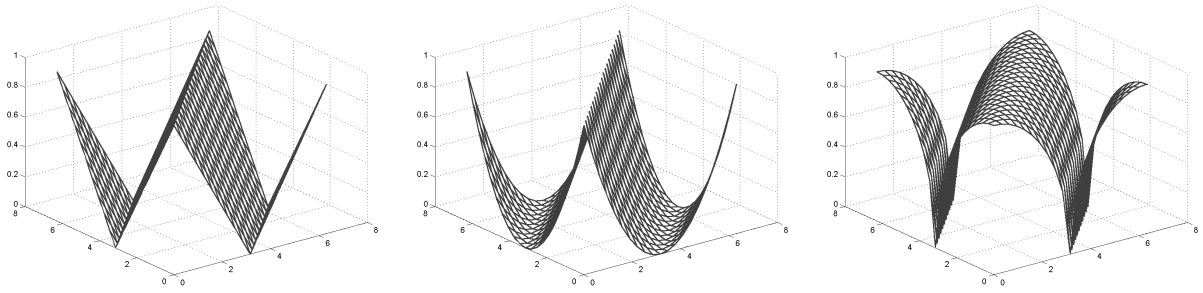

(a) $\varphi(x) = x$, $\psi(x) = x$ (b) $\varphi(x) = x$, $\psi(x) = \sqrt{\pi x}$ (c) $\varphi(x) = x^2$, $\psi(x) = \frac{x^2}{\pi}$

Figure 3: Restricted radial equivalence functions created as in Proposition 4 from automorphisms in the unit interval (φ) and in $[0, \pi]$ (ψ).

(RR5) For all $a, b, c, d \in \Omega$, if $d(b, c) \leq d(a, d)$, then $r_\theta(b, c) \geq r_\theta(a, d)$.

Definition 7 is not a direct extension of Definition 2 to radial data. The differences arise from the use of distances in (RR5) instead of orders (as in (R5)). Nevertheless, this change is due to the difficulties in the interpretation of orders in radial universes. Despite this modification, we believe that the spirit and semantics of RREFs are those of REFs.

In this work, we only consider RREFs associated with the angular metric $d^*(a, b) = \min(|b - a|, 2\pi - |b - a|)$ but many other metrics are also eligible, e.g.:

$$d(a, b) = \begin{cases} 0 & \text{if } a = b, \\ \pi & \text{if } d^*(a, b) = \pi, \\ \pi/2 & \text{otherwise.} \end{cases}$$

Proposition 3. *Let r_θ be a RREF associated with the metric d^*. For all $a_1, b_1, a_2, b_2 \in \Omega$, if $d^*(a_1, b_1) = d^*(a_2, b_2)$ then $r_\theta(a_1, b_1) = r_\theta(a_2, b_2)$.*

Proof. *Let $a_1, b_1, a_2, b_2 \in \Omega$ such that $d^*(a_1, b_1) = d^*(a_2, b_2)$. According to (RR5), $d^*(a_1, b_1) \leq d^*(a_2, b_2)$ implies $r_\theta(a_1, b_1) \geq r_\theta(a_2, b_2)$. Analogously, $d^*(a_2, b_2) \leq d^*(a_1, b_1)$ implies $r_\theta(a_2, b_2) \geq r_\theta(a_1, b_1)$ so the equality holds.*

Corollary 1. *Let $h : \Omega^2 \to [0, 1]$. If h satisfies (RR5) with respect to the metric d^* then it also satisfies (RR4).*

Proof. *Trivial by Proposition 3 since $d^*(a, b) = d^*(m(a), m(b))$.*

Following the construction of REFs, we also define a new possible construction method for RREFs, which is also based on automorphisms.

Proposition 4. *Let φ and ψ be automorphisms of the intervals $[0, 1]$ and $[0, \pi]$, respectively. The mapping $t : \Omega^2 \to [0, 1]$ given by*

$$t(a, b) = \varphi^{-1}\left(1 - \left(\frac{1}{\pi}\psi\left(d^*(a, b)\right)\right)\right) \tag{3}$$

is a RREF.

Proof. *Direct by the properties of the metric d^*.*

Some examples of RREFs constructed as in Proposition 4 are included in Fig. 3.

3.2. Radial Similarity Measures

Definition 8. *A mapping $s_\theta : \Omega^k \times \Omega^k \to \mathbb{R}^+$ is said to be a k-ary Radial Similarity Measure (RSM) associated with the metric d^* if it satisfies the following:*

(SR1) $s_\theta(\boldsymbol{a}, \boldsymbol{b}) = s_\theta(\boldsymbol{b}, \boldsymbol{a})$ for all $\boldsymbol{a}, \boldsymbol{b} \in \Omega^k$;

(SR2) $s_\theta(\boldsymbol{a},\boldsymbol{b}) = 0$ *if and only if* $d^*(a_i,b_i) = \pi$ *for all* $i \in \{1,\ldots,k\}$*;*

(SR3) $s_\theta(\boldsymbol{c},\boldsymbol{c}) = Max_{\boldsymbol{a},\boldsymbol{b}\in\Omega^k} s_\theta(\boldsymbol{a},\boldsymbol{b})$ *for all* $c \in \Omega^k$*;*

(SR4) For all $\boldsymbol{a},\boldsymbol{b},\boldsymbol{c},\boldsymbol{d} \in \Omega^k$*, if* $d^*(\boldsymbol{a},\boldsymbol{d}) \geq d^*(\boldsymbol{b},\boldsymbol{c})$ *then* $s_\theta(\boldsymbol{a},\boldsymbol{d}) \leq s_\theta(\boldsymbol{b},\boldsymbol{c})$*, where* $d^*(\boldsymbol{a},\boldsymbol{d}) \geq d^*(\boldsymbol{b},\boldsymbol{c})$ *implies that* $d^*(a_i,d_i) \geq d^*(b_i,c_i)$ *for all* $i \in \{1,\ldots,k\}$.

RSMs can be constructed from RREFs, aggregating their results over each element, as it is done for SMs.

Proposition 5. *Let* r_θ *be a RREF and let* f *be a* k*-ary aggregation function such that* $f(\boldsymbol{x}) = 0$ *if and only if* $x_i = 0$ *for all* $i \in \{1,\ldots,k\}$ *and* $f(\boldsymbol{x}) = 1$ *if and only if* $x_i = 1$ *for all* $i \in \{1,\ldots,k\}$*. The function* $s_{\theta_{[f,r_\theta]}} : \Omega^k \times \Omega^k$*, given by*

$$s_{\theta_{[f,r_\theta]}}(\boldsymbol{a},\boldsymbol{b}) = f(r_\theta(a_1,b_1),\ldots,r_\theta(a_k,b_k)) \tag{4}$$

is a k*-ary radial similarity measure that satisfies*

- $s_{\theta_{[f,r_\theta]}}(\boldsymbol{a},\boldsymbol{b}) = s_{\theta_{[f,r_\theta]}}(\boldsymbol{b},\boldsymbol{a})$ *for all* $\boldsymbol{a},\boldsymbol{b} \in \Omega^k$*;*
- $s_{\theta_{[f,r_\theta]}}(\boldsymbol{a},\boldsymbol{b}) = 0$ *if and only if* $d^*(a_i,b_i) = \pi$ *for all* $i \in \{1,\ldots,k\}$*;*
- $s_{\theta_{[f,r_\theta]}}(\boldsymbol{a},\boldsymbol{b}) = 1$ *if and only if* $a_i = b_i$ *for all* $i \in \{1,\ldots,k\}$*;*
- *For all* $\boldsymbol{a},\boldsymbol{b},\boldsymbol{c},\boldsymbol{d} \in \Omega^k$*, if* $d^*(\boldsymbol{a},\boldsymbol{d}) \geq d^*(\boldsymbol{b},\boldsymbol{c})$ *then* $s_{\theta_{[f,r_\theta]}}(\boldsymbol{a},\boldsymbol{d}) \leq s_{\theta_{[f,r_\theta]}}(\boldsymbol{b},\boldsymbol{c})$*, where* $d^*(\boldsymbol{a},\boldsymbol{d}) \geq d^*(\boldsymbol{b},\boldsymbol{c})$ *implies that* $d^*(a_i,d_i) \geq d^*(b_i,c_i)$ *for all* $i \in \{1,\ldots,k\}$.
- $s_{\theta_{[f,r_\theta]}}(\boldsymbol{a},\boldsymbol{b}) = s_{\theta_{[f,r_\theta]}}(m(\boldsymbol{a}),m(\boldsymbol{b}))$ *for all* $\boldsymbol{a},\boldsymbol{b} \in \Omega^k$ *where* $m(\boldsymbol{a}) = (m(a_1),\ldots,m(a_k))$.

4. Template-based singular point detection

In this section we present a SP detection method based on RSMs and RREFs. Section 4.1 introduces the problem of SP detection, while Section 4.2 presents the template based SP detection method and Section 4.3 outlines the resulting algorithm.

4.1. Fingerprint classification and singular point detection

Fingerprint-based identification is the most popular type of biometrical identity authentication systems. These systems carry out the authentication analysing the ridge patterns in the surface of the fingertips. There are two main tasks that can be performed in the context of fingerprint analysis, namely *identification* and *verification*. The former term refers to the localization of an individual in a database by the usage of an input fingerprint. The latter term refers to confirming whether an input fingerprint corresponds to a certain individual in the database. In both cases, having an accurate way to perform one-to-one fingerprint comparisons is critical [31].

The most common approach to decide whether two fingerprints are produced from the same fingertip is to compare local ridge features, usually, the so-called *minutiae*, which are local discontinuities or anomalies in the ridge pattern [32, 33]. Examples of minutiae are ridge breaks and bifurcations. The whole process of deciding whether two fingerprints belong to the same individual is known as *matching* [34, 35, 31, 36].

Fingerprint matching is not trivial, and very often demands a certain computational effort. This is not a problem in fingerprint verification (since the input fingerprint is only compared with those corresponding to the claimed identity), but it becomes critical in fingerprint identification. For this reason, several strategies have been developed to minimize the number of comparisons to be performed. Among them, the most used one is *classification* [16, 37, 38], which consists of classifying each fingerprint according to the general structure of its ridges. In this way, when an input fingerprint has to be matched, it only need to be compared with those belonging to the same class. Although different classification schemes for fingerprints have been proposed, most of the authors in fingerprint analysis use the five major classes in the Henry system [39], namely *arch*, *tented arch*, *left loop*, *right loop*, *whorl*. Examples of these five classes can be found in Fig. 4. As a result of this division, the number of comparisons in an identification process can be drastically reduced. Nonetheless, this task also holds great responsibility. If a fingerprint is misclassified, the

(a) Arch (b) Tented Arch (c) Left loop (d) Right loop (e) Whorl

Figure 4: Examples of fingerprint for each of the five classes in the Henry classification system. These fingerprints have been created using the SFinGe tool [40, 39].

system will not be able to perform a correct identification or it may lead to an increase in the computational effort due to the greater number of comparisons that must be carried out.

Fingerprint classification is often defined as the problem of learning a classifier able to determine the class to which a (previously unseen) fingerprint belongs to. In order to do so, the classifier is usually learned from a set of labelled fingerprints. Fingerprints are classified using global features from the ridge flow, instead of local ones as it is done in fingerprint matching. Hence, fingerprint classification consists of two well-differentiated steps[3]: (a) feature extraction, where fingerprints are processed to obtain their feature vector, and (b) classification, where a classifier associates such vector to one of the classes. In this work we focus on the first one; more specifically, on the detection of the so-called singular points (SPs), which are the most commonly used feature for classification.

SPs are locations of the fingerprint in which abnormal ridge patterns occur. In a fingerprint, two types of SPs can be found: *cores* (where ridges tend to converge) and *deltas* (where the ridge flow diverges). The importance of these features for classification is clear, given that the classes in the Henry system can indeed be described in terms of SPs:

- *Arch*: There are no SPs, since the ridges flow horizontally producing a small bump in the center of the fingerprint.
- *Tented Arch*: There is one core and one delta, and the delta is under the core. The ridge flow is similar to that of the Arch type, but at least one ridge shows high curvature.
- *Left Loop*: One core and one delta, and the delta is underneath and on the right of the core. One or more ridges flow from the left side, curve back, and disappear again to the left margin of the fingertip.
- *Right Loop*: There is one core and one delta, and the delta is underneath and to the left of the core. One or more ridges flow from the right side, curve back, and disappear again on the right margin of the fingertip.
- *Whorl*: There are two cores and two deltas, and at least one of its ridges makes a full turn around the center of the fingerprint.

A proper description of SPs might be sufficient for the classification of a fingerprint, by using a fixed rule-based strategy [17, 41]. Still, learning-based approaches to classification have also been proposed [42, 43, 21]. In general, it is accepted that accurate SP detection is required in order to reach the highest possible accuracy in the posterior classification process. Note that, apart from their relevance in fingerprint classification, SPs are also used for some other processes on fingerprints, e.g. fingerprint alignment with respect to a reference point [44] (usually a core point).

Despite the importance of SPs, their extraction is still an open problem for which proposals are constantly being presented [16, 45, 46]. Most of such proposals are based on the semi-local analysis of the so-called Orientation Map (OM), which is a block-based description of the ridge flow in a fingerprint [47] (see Fig. 5(b) for an example). The most relevant proposal for SP detection is the Poincarè method [20]. In this method, each of the blocks in the orientation map is assigned a Poincarè index, which is computed as the total rotation of the orientations around it. This index determines the presence of a SP, as well as its type (*i.e.*, either core or delta). A popular approach, also based on OMs, is the one proposed by Nilsson and Bigun [18]. Additionally to the usage of complex filters, an interesting

[3] We refer to [16, 37] for a detailed review on the topic.

novelty in [18] resides in the use of *Squared OMs* (SqOM) [48], which are obtained by multiplying by 2 the orientation at each block of an OM. This simple representation of the OM has the key advantage of producing rotation-invariant patterns at SP locations. Fig. 5 illustrates how SPs look in both conventional and squared orientation maps.

In our SP detection framework we aim at exploiting the high visibility of SPs in squared OMs. More specifically, we propose to use a template-based approach to SP detection which consists of comparing templates of SPs with the actual occurrences of SqOMs. In this context, RREFs and RSMs become crucial, allowing the comparison of the directions in the SqOMs with those in the templates. Forthcoming sections provide details on our method.

4.2. Template-based singular point detection

Template matching procedures are recurrent solutions in digital image processing. The reason is that the only a priori information needed for such procedures is an expression of the goal (which stems from the definition of the problem) and a comparison measure able to quantify the similarity between the input data and the template. Examples of template based methods for image processing are some low-level feature detectors [49, 50, 51], or composite object detectors (e.g. the eye detector in [52]). Moreover, despite template matching is conceptually simple, it has also evolved into rather complex theories, among which we can list, for example, mathematical morphology [53].

In this section we present a framework for SP detection based on templates, which is referred to as *Template-based SP Detection* method (TSPD method). To the best of our knowledge, no author has proposed to use templates to represent SPs, probably due to the lack of reliable comparison methods that can handle the matching score. The most similar approach is the usage of complex filters [21], which are convolved with the complex representation of the OM. Notice that we also include this method as baseline performer in the experiments. From our point of view, template-matching is a natural way to search for SPs, as long as the definition of SP is vague and based on human perception.

Any template matching-based framework is composed of three nuclear components: (a) an appropriate representation of the input data, (b) templates describing the patterns to be searched in terms of the input data, and (c) a reliable tool to quantify the similarity between both representations. Since our framework is deeply based on mimicking human perception, our aim is to maintain all three components as faithful as possible to the human comprehension of the problem. Consequently, we elaborate on the ridge-like representation of fingerprints (a) and templates (b), while employing RSMs for (c).

(a) *Fingerprint representation using orientation maps.*- The most obvious representation for SP detection is the fingerprint image itself, since that is all the information humans need to locate SPs. However, this representation is inconvenient, and would dramatically hinder the representation of the template. The reason is that, despite the fact that humans take as input the original image, the location of SPs is based on the analysis of the ridges. That is, the humans automatically convert the tone-based representation of the fingerprint into a ridge-based one.

The representation of the ridges in an image has been often studied, and most of the authors agree on using OMs [47]. These maps divide the fingerprint images into disjoint blocks, assigning to each of them a unique orientation given by the majority ridge orientation of its pixels. The best-known approach to OM extraction is the gradient method [45]. In this method, the orientation of the ridges is computed pixel-wise as the perpendicular to the gradient direction. In Fig. 5 we display the OM of a whorl type fingerprint. We observe how cores take oriented cup-like patterns, which are dependent on the specific orientation of each SP, and deltas produce triangular orientation patterns.

In this work we use the SqOMs, which are better fitted than OMs to our goals. This representation, as shown in Fig. 5, produces interesting changes in the representation of SPs. More specifically, it creates a rotation-invariant representation of cores, which are represented as either clockwise or anticlockwise streams. Regarding deltas, the situation is not as positive, since their appearance does not become rotation-invariant. In any case, using SqOMs simplifies the design of the templates, and is kept as standard representation in our framework.

(b) *Templates for SP representation.*- The templates in our framework must be a minimal set such that it completely captures the way in which SPs appear (or are perceived) in a SqOM. Cores manifest themselves as either clockwise or anticlockwise sequences of orientations, so there is only need for two templates. Moreover, these templates can be functionally represented in a very simple manner.

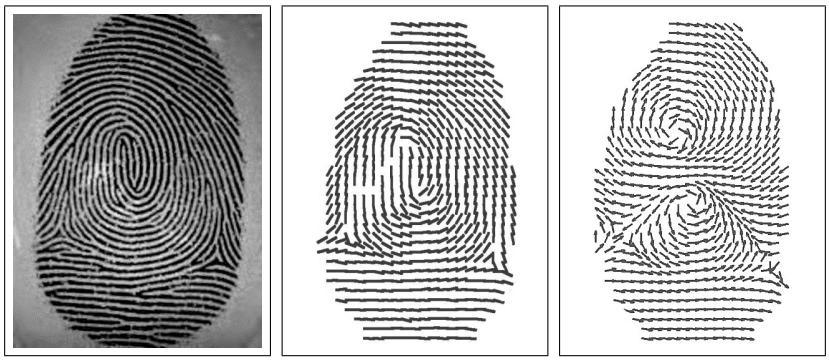

(a) (b) (c)

Figure 5: Whorl image generated with SFinGe (a), together with its Orientation Map (OM) (b) and Squared Orientation Map (SqOM) (c). We have considered a size of block of 12×12 pixels to optimize the visibility of each block.

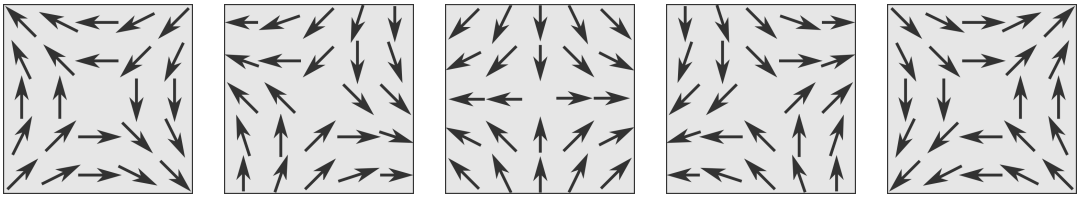

(a) $T_{\alpha=0}$ (b) $T_{\alpha=\frac{\pi}{8}}$ (c) $T_{\alpha=\frac{\pi}{4}}$ (d) $T_{\alpha=3\frac{\pi}{8}}$ (e) $T_{\alpha=\frac{\pi}{2}}$

Figure 6: Examples of delta SP templates generated as in Eq. (6) with different values of α.

Let the origin $(0, 0)$ represent the center of a template T of size $(2n + 1) \times (2n + 1)$. The orientation at a position $(x, y) \in [-n, n]^2$ of a core template is given by

$$T(x, y) = \begin{cases} \mathrm{atan2}(y, x) & \text{if it is a clockwise core, and} \\ \mathrm{atan2}(-y, -x) & \text{if it is an anticlockwise core,} \end{cases} \tag{5}$$

where $\mathrm{atan2}(y, x)$ is the well-known sign-sensitive version of the arctangent of $\frac{y}{x}$, *i.e.*, the angle of the vector (x, y) with respect to the positive x-axis. Note that the center of the template has no value, and hence contains no information for the matching process.

With respect to deltas, the problem becomes trickier. In a general manner, a delta is represented as a triangular pattern in the OM, and becomes a symmetric pattern with vectors opposing each other in two orthonormal directions in the SqOM (see Fig. 5). None of those representations is rotation invariant, and consequently an orientation-dependent template must be created to represent delta SPs. The orientation at a position $(x, y) \in [-n, n]^2$ of a delta SP template with orientation $\alpha \in [0, \pi]$ is given by

$$T_\alpha(x, y) = \mathrm{atan2}(-(\cos(\alpha)y - \sin(\alpha)x), \sin(\alpha)y + \cos(\alpha)x) \; . \tag{6}$$

Figure 6 displays the delta SP template for different values of α. In such images we can observe how the pattern is composed of two orthonormal axis, one acting as an *attractor* to the origin, the other one being a *repeller* to it.

According to the previous template definitions, there are two decisions to be made on the set of templates. The first decision affects the number of delta SP templates to be used, *i.e.* the number of different values of α to produce a pattern. One can foresee that a greater number of templates will lead to more accurate detections, although it might also lead to a better fitting of abnormal ridge occurrences that do not correspond to SPs as well as a higher computational effort. The second decision relates to the size of the templates. Indeed the size of the templates must be dependent upon the size of the blocks in the SqOM, as well as upon the expected granularity of the fingerprint capturing process. These parameters are discussed in Section 5.3.

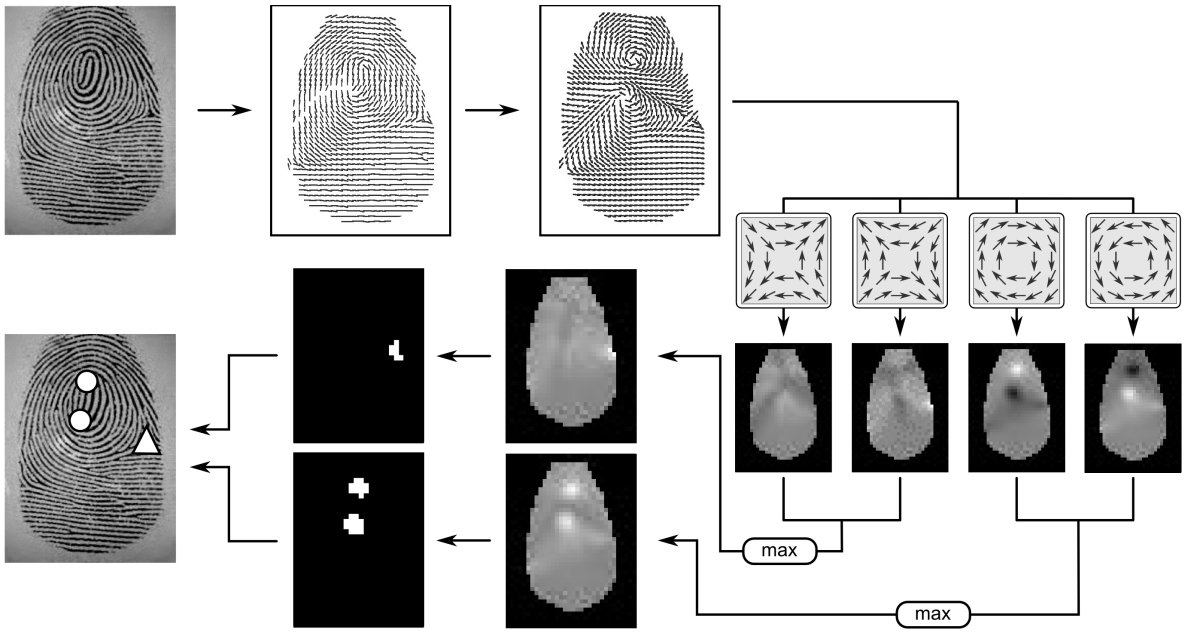

Figure 7: Schematic representation of the proposed framework for singular point detection using orientation templates and radial similarity measures, namely Template-based singular point detection (TSPD).

(c) *Comparison of SqOMs and templates.*- The comparison of SqOMs and templates is done in the simplest possible manner. For each template we produce a similarity map with the same dimensions as the SqOM. Each position of such similarity maps corresponds to the value yielded by the RSM between the template and the neighbourhood of the block. Finally, all the similarity maps corresponding to the same type of SP are fused using the $\max$ operator. In this way, we obtain two graded representations of the presence of SPs, one for each type of SP.

4.3. Proposed algorithm

The ideas in Section 4.2 outline the complete algorithm for the detection of SPs in fingerprints.

Note that the algorithm is presented without giving the specific parameters used to make it as general as possible. Furthermore, these parameters must be chosen depending on the characteristics of the images in which it is applied. For this reason, the complete parameter specification used in this paper is shown in Section 5.3. This algorithm is composed of the following phases, which are also schematically represented in Fig. 7:

1. Dividing the image into non-overlapping blocks.
2. Segmenting the image using the previous calculated blocks.
   - 2.1.- Normalizing the image to a desired mean and variance, 100 and 1000, respectively [33].
   - 2.2.- Segmenting the fingerprint and the background, by assigning to the latter those blocks for which the variance of the pixel intensities is greater than 30 [33].
3. Calculating the orientation map over the segmented image.
   - 3.1.- Computing the gradient at each pixel of the image (e.g., using Sobel masks) [45].
   - 3.2.- Since the gradients are computed for each pixel and the result of a single pixel may not be reliable enough, the OM is smoothed to get more accurate orientations. In order to do so, the technique by Kass and Witkin [48] is used.
   - 3.3.- Creating the OM from the regularized orientations.

4. Creating the SqOM by multiplying by two the values in the OM.

5. Detecting singular points.

   5.1.- Computing the similarity map for each template. This is done by comparing the elements of the SqOM and those in each templates using the RSMs in Section 3.2.

   5.2.- Fusing the similarity maps corresponding to each type of SP. This is done by obtaining, at each block, the maximum response for the cores and, in parallel, for the deltas.

   5.3.- Selecting cores and deltas. This is done by taking the two points with the highest local response for core and delta similarity map in parallel. They are considered as a SP if they overall a threshold (Table 2).

Regarding computational times of the new technique, it is worth mentioning that it is comparable to the others methods we have used, Liu and Poincarè. All the methods compared share the same computational process. They go trough the fingerprint image executing a series of operations to get local maximums (SPs). One of the differences between the new method and Liu's method is that it does not use multi-scale image processing. This leads to a speed increase in execution time, but we consider it negligible. The segmentation step and the creation of the OM are common to all the methods and the complexity of the singular point extraction is equivalent to Liu's method. It may be a slight increase in complexity but it is imperceptible.

5. Experiments

The TSPD method has qualitative advantages compared to other traditional methods, e.g., the simplicity of the process and its visualization. However, it also demands a quantitative verification. In this section we check the quantitative performance of our method compared to that of the most relevant SP detection methods in the literature. In Section 5.1, we review the datasets we have used in the comparison. Section 5.2 covers the details on the quantification of the results, whereas Section 5.3 contains a detailed review of the setting and parametrization of the SP detection methods. The results, as well as a brief discussion, are included in Section 5.4.

5.1. Datasets

This experiment uses fingerprints from two different sources. The first one is National Institute of Standards and Technology Special Database 4 (NIST-4) [19]. This database contains rolled-ink fingerprints from the FBI (Federal Bureau of Investigation) and is, historically, the most used benchmark in the fingerprint classification literature. NIST-4 contains 4000 fingerprints (of 512×480 pixels) taken from 2000 fingertips. Hence, there are two captions of each fingerprint. Note that in NIST-4, as well as in most of the available databases, there is no ground truth with respect to the position and type of the SPs. On this account, we have manually labelled the first 1000 fingerprints from NIST-4 database to evaluate the proposed method. Labelling has been carried out according to the specifications given in the specialized literature and has been thoroughly revised by multiple reviewers. In order to ease the process of evaluating further proposals, our ground truth is available at [54]. For illustrative purposes, Fig. 1 shows three fingerprints from NIST-4, together with the corresponding ground truth data.

Even though NIST-4 is widely accepted, it should also be mentioned that in this dataset fingerprint classes are evenly represented, contrary to the reality in real-world databases, in which their distribution is skewed. Moreover, the representation of rolled-ink captions is limited, since most of the current applications collect fingerprint images using optical sensors. For these reasons, we also consider three additional databases generated with SFinGe synthetic fingerprint generator [40, 39]. Although synthetic, SFinGe-generated fingerprints reflect in a faithful manner the difficulties in real scenarios. Moreover, the class distribution can be adjusted to that in reality, that is, 3.7%, 2.9%, 31.7%, 33.8% and 27.9% for arch, tented arch, right loop, left loop and whorl, respectively. Finally, it is relevant that SFinGe itself provides the ground truth data for the SPs, and hence the evaluation process becomes completely objective, whereas in NIST-4 there may be a certain error due to the manual labelling. The validity of the fingerprint images produced by SFinGe is, in any case, widely accepted, to the point that it has already been used in several editions of the Fingerprint Verification Competition (FVC) [55, 56, 57, 58, 59] with results similar to those obtained with real fingerprint databases.

Scanner parameters
Acquisition area: 0.58" × 0.77" (14.6mm × 19.6mm) Resolution: 500 dpi, Image size: 288 × 384 Background type: Optical Background noise: Default Crop borders: 0 x 0
Generation parameters
Seed: 1 Impression per finger: 25 (only the first one is used) Class distribution: Natural Generate pores: enabled Save ISO templates: enabled
Output settings
Output file type: WSQ

Table 1: Setting of SFinGe for the generation of the three datasets used in the experimental validation.

(a) Profile *HQNoPert* (b) Profile *Default* (c) Profile *VQandPert*

Figure 8: Fingerprints generated using SFinGe with different quality profiles .

Aiming at simulating different scenarios, we have used three different quality profiles in the generation of fingerprints with SFinGe. For each quality profile, we generate 1000 fingerprint images. The following profiles are considered in our experiments (the rest of the parameters used in SFinGe tool are presented in Table 1):

- *High Quality No Perturbations* (HQNoPert): High quality fingerprints without any kind of perturbation;
- *Default*: Middle quality fingerprints with slight localization and rotation perturbations;
- *Varying Quality and Perturbations* (VQandPert): Fingerprints with different qualities are included, which are perturbed in location, rotation and geometric distortions.

The fingerprints generated for each quality profile are rather different, and also significantly different from those in NIST-4. Fig. 8 includes one fingerprint for each of the above mentioned quality profiles. In the remainder of this work, we refer to the datasets created with profiles HQNoPert, Default and VQandPert as SFinGe Dataset 1, 2 and 3, respectively.

5.2. Quantification of the results

In this experiment we have quantified the performance of each procedure in correctly and accurately detecting SPs. For each dataset we have created a confusion matrix which accounts for the success and fallout in SP detection. That is, given a dataset, a unique confusion matrix is completed from the confrontation of the SPs detected by the automatic method at each image and those in the ground truth.

After extracting the SPs for a fingerprint, we first compute the best-possible matching between the cores in the automatic solution to those in the ground truth, forcing a one-to-one correspondence. Each matched core in the automatic solution accounts for as True Positive (TP). Then, each unmatched core in the automatic solution and in the ground truth are tagged as False Positive (FP) and False Negative (FN), respectively. Finally, in case both the automatic solution and the ground truth contain less than two cores, the missing SPs are taken as correct predictions,

and consequently are accounted for as True Negatives (TN). The process is analogous for the deltas, whose results are stored in a separate matrix. Note that each fingerprint can generate more than two hits in the confusion matrix, if SPs are both missed (FNs) and misdetected (FPs).

It should be considered that fingerprint analysis methods do not necessarily locate a SP at the exact location a human does. This is due to the discrete nature of data in an image and the scope of the semi-local analysis of the image needed to locate the SPs. Consequently, we consider some tolerance in the correspondence of SPs tagged by the automatic method to those in the ground truth. For the present experiment, this spatial tolerance is equivalent to 5% of the image diagonal for SFinGe databases and 10% of the image diagonal for NIST-4 database. The percentage difference between databases arises from the size of SFinGe and NIST-4 fingerprints (SFinGe ones are rectangular images, whereas NIST-4 ones are squared, but also the thickness of the ridges vary due to their different nature).

The results generated with the above-mentioned procedure lead to two confusion matrices for each dataset, one for cores and one for deltas. From such matrices, we have generated different scalar interpretations of the quality of the results. More specifically, we consider precision (PREC) and recall (REC), given by

$$\text{PREC} = \frac{\text{TP}}{\text{TP}+\text{FP}} \text{ and } \text{REC} = \frac{\text{TP}}{\text{TP}+\text{FN}}, \tag{7}$$

respectively. Precision and recall quantify the ability of the automatic method to obtain a reliable and complete collection of SPs, respectively. They can be combined to produce a scalar representation of the overall quality of the process. In this work we adhere to the so-called F-measure, given by

$$\text{F} = \frac{\text{PREC} \cdot \text{REC}}{0.5\,\text{PREC} + 0.5\,\text{REC}}\ . \tag{8}$$

Moreover, we also measure the percentage of fingerprints in which all the SPs (cores and deltas) have been correctly detected.

5.3. Experimental procedure

In this experiment, the results of the TSPD method have been compared with those of the Poincarè method [20], as well as to those of the one proposed by Liu [21]. The former method has been selected because it is the most used SP detection method in literature, whereas the latter method is included because it holds strong similarities to ours. Aiming at carrying out a fair comparison, the techniques used for OM computation, smoothing and segmentation are identical for each of the three SP detection methods.

Firstly, the image is divided into non-overlapping blocks of 5×5 pixels (for SFinGe databases) or 10×10 pixels (for the NIST-4 database). The different size between SFinGe and NIST-4 fingerprints makes it necessary to use different block sizes, since the ridges of the NIST-4 fingerprints are much thicker than SFinGe ones. Secondly, the image is segmented (as explained in Section 4.3) to avoid false SP detections in the ridge abnormalities occurring at the fingertip boundaries. Thirdly, to compute the gradients for the OM we use the well-known Sobel operators [60, 61], which is the most common option in fingerprint analysis. The resulting matrix is the OM, which is further regularized using a flat mask of 5×5 blocks [48]. Notice that we do not use a different size of mask for NIST-4 fingerprints since the block size used to compute the OM produces blocks with equivalent information regardless of the database.

Once the OM is generated, each of the methods needs to be customized, the details being as follows:

- *TSPD*– Regarding the templates, we need to set their size and the number of delta SP templates to use. In order to preserve the fairness of the comparison, we have considered a very basic setup, which is the baseline configuration of the method. This configuration involves only 4 templates (two for each type of SP), all of them of 5×5 blocks. In the case of the delta SP templates, we take $\alpha \in \{0, 90\}$. This is, objectively, the minimum set of templates to be used.

  As for the RSMs, we consider 9 measures, in order to shed light on the impact the RSMs have on the final results. This way, we are able to show their flexibility, allowing one to define different perceived similarities. The RREFs are constructed as in Prop. 4 from pairs of automorphisms (φ, ψ) given by

$$\varphi(x) = x^{e_1} \text{ and } \psi(x) = \frac{x^{e_2}}{\pi^{e_2-1}}$$

Name	e_1	e_2	Threshold
C1	0.5	0.5	0.70
C2	0.5	1.0	0.85
C3	0.5	2.0	0.95
C4	1.0	0.5	0.55
C5	1.0	1.0	0.70
C6	1.0	2.0	0.85
C7	2.0	0.5	0.35
C8	2.0	1.0	0.60
C9	2.0	2.0	0.75

Table 2: List of configurations of the TSPD used in the experimental validation. For each of the configurations, we list the exponents (e_1, e_2) of the automorphisms used in the construction of the RREF, as well as the threshold used for SP discrimination.

where $e_1, e_2 \in \{0.5, 1, 2\}$. This leads to 9 different pairs of automorphisms.

Each combination of automorphisms, together with the thresholds used for the discrimination of the SPs, is shown in Table 2. Although some authors have studied the automatic determination of thresholds [62, 63], we avoid this step in order to preserve the clarity and reproducibility of the experiments. Several thresholds have been tested before selecting one that has a positive behaviour in all datasets (see Table 2).

- *Poincarè method*– This method consists of computing the difference between each orientation in a 3×3 neighbourhood and its clockwise successor. Those differences are further summed up to produce the Poincarè index in each block. This index takes value 0, $\frac{1}{2}$ or $-\frac{1}{2}$, indicating the absence of a SP, the presence of a core or the presence of a delta, respectively. Although other authors have used other configurations of the neighbourhood [17, 64], specially regarding its size, we maintain the widely accepted 3×3 size.

- *Liu's method*– In this method the SqOM is filtered with first order complex filters at different scales. More specifically, the large scale filters are used to discriminate the real SPs from spurious responses, while the fine scale ones determine their precise location. The threshold used for discrimination of SPs is set to 0.7 (this threshold is manually set to measure the performance of the method, as those in Table 2). Regarding the scales we consider, as in [21], filters of $s \times s$ blocks, with $s \in \{3, 5, 7, 9\}$.

5.4. Results

The results obtained for each method and dataset are listed in Tables 3-6, including:

- The values at each position of the confusion matrix (as explained in Section 5.2), namely PREC, REC and F. This information is displayed for cores and deltas separately.

- The average distance in pixels from the position at which the matched SPs where located and their position at the ground truth. This information is also listed individually for cores and deltas.

- The arithmetic mean between the F value for cores and deltas, namely Combined F (Comb. F).

- The percentage of fingerprints for which the method achieved a perfect detection (Perfect Detection Percentage, PDP). That is, the rate of fingerprints for which each method gathered the exact number of SPs, all of them being located within the tolerance ratio of 5% and 10% of the length of the image diagonal, for SFinGe and NIST-4 fingerprints, respectively.

For each dataset, the best performer at each statistic is boldfaced.

The first fact to be noticed from the results of the experiment is the great variability of performance across datasets, especially between NIST-4 and SFinGe datasets. This is due to the low quality of NIST-4 fingerprints, which often include damaged fingertips, hand-written annotations on the fingerprint margins, etc. This does not reduce the representativity of the datasets generated with SFinGe, since modern sensors for fingerprint recording produce images

Quant.	Template-based SP detection C1	C2	C3	C4	C5	C6	C7	C8	C9	Poincaré	Liu
Cores											
TP	897	875	868	853	911	912	867	850	915	759	**922**
FP	273	147	132	161	266	241	292	138	261	**40**	329
FN	93	115	122	137	79	78	123	140	75	231	**68**
TN	776	889	905	878	777	799	756	902	782	**982**	721
PREC	.767	.856	.868	.841	.774	.791	.748	.860	.778	**.950**	.737
REC	.906	.884	.877	.862	.920	.921	.876	.859	.924	.767	**.931**
F	.831	.870	**.872**	.851	.841	.851	.807	.859	.845	.849	.823
Avg. dist.	14.4	**13.7**	13.8	14.9	14.2	14	15.6	14.3	13.9	13.8	16.4
Deltas											
TP	871	844	839	830	874	877	814	837	**881**	728	767
FP	340	176	159	188	393	351	335	163	426	53	**29**
FN	102	129	134	143	99	96	159	136	**92**	245	206
TN	731	884	898	879	682	722	754	897	648	1006	**1011**
PREC	.719	.827	.841	.815	.690	.714	.708	.837	.674	.932	**.964**
REC	.895	.867	.862	.853	.898	.901	.837	.860	**.905**	.748	.788
F	.798	.847	.851	.834	.780	.797	.767	.848	.773	.830	**.867**
Avg. dist.	11.2	10.4	**10.3**	11.3	11.1	10.6	12.1	11	10.7	13.5	11.5
Total											
Comb. F	.815	.859	**.861**	.843	.811	.824	.787	.853	.809	.839	.845
PDP	56.70	68.10	**69.90**	63.00	54.50	58.70	48.10	66.90	52.80	66.40	54.50

Table 3: Results gathered by each SP detection method on the NIST-4 dataset (1000 fingerprints).

that are closer to those by SFinGe than to those in NIST-4. This variable behaviour has also been shown in previous studies on the topic [37].

Regarding the NIST-4 dataset, we find that TSPD-C3 is the best performer, obtaining the greatest PDP (69.90%). Although TSPD-C2 and TSPD-C8 stay close to this result, configurations such as TSPD-C7, TSPD-C9 and TSPD-C5 lead to the worst outcome. The relevance of the RSMs is clearly illustrated with these results. Besides, TSPD-C5 (when φ and ψ are the identity function) is not the best performer. From this fact, we infer that choosing suitable automorphisms on the construction of the RREFs significantly improves the result of the TSPD method. In Table 3 we also observe that Liu's method obtains a PDP similar to our worst configurations (54.50%). Despite being the best method detecting cores (922), Liu's method also produces 329 false cores detections, significantly more than the Poincarè method (40) and TSPD-C3 (132). The behaviour is opposed regarding deltas, where the precision of Liu's method is very high (29 FPs and 1011 TNs), at the cost of very little recall (767 TPs)[4]. Otherwise, the method of Poincarè presents a high PDP, but is not the best performer because of its difficulties in detecting cores (231 FNs) and deltas (245 FNs). From this results, we understand that TSPD-C3 obtains the best results in general terms, showing the most equilibrated behaviour between successes (TPs, TNs) and failures (FPs, FNs).

For the SFinGe datasets, we observe that in Table 4 and Table 5, TSPD-C3 obtains the best PDP results (95.90% and 88.50% respectively), although in Table 6 the best one is TSPD-C6 (90.00%). The general trend observed in Tables 4-6 is that the TSPD method is usually able to outperform both the Poincarè and Liu's methods, although certain configurations fail to do so. A remarkable fact is the absolute absence of core FPs when using the TSPD method, which hardly ever account for more than 30 of such mistakes over 1000 fingerprints. This leads to high PREC and, as a consequence, to high F. The situation with the delta SPs is similar as it is for core SPs, but not as positive for the TSPD method. In Dataset 1, the results are similar to those of the cores, but the situation changes in Dataset 2 and is accentuated in Dataset 3.

Summing up, from the results in the present experiment we consider the TSPD method to be competitive with the contending methods. Although the TSPD method requires setting the parameters of the RSMs and thresholds, similar

[4]This behaviour of Liu's method is consistent with that observed by Galar *et al.* [37]

	Template-based SP detection									Poincaré	Liu
Quant.	**C1**	**C2**	**C3**	**C4**	**C5**	**C6**	**C7**	**C8**	**C9**		
Cores											
TP	1209	1215	1228	1157	1216	1230	1151	1165	1228	1187	**1232**
FP	1	**0**	1	**0**	**0**	**0**	16	**0**	3	**0**	58
FN	33	27	14	85	26	12	91	77	14	55	**10**
TN	757	**758**	757	**758**	**758**	**758**	742	**758**	756	**758**	702
PREC	.999	**1**	.999	**1**	**1**	**1**	.986	**1**	.998	**1**	.955
REC	.973	.978	.989	.932	.979	.990	.927	.938	.989	.956	**.992**
F	.986	.989	.994	.965	.989	**.995**	.956	.968	.993	.977	.973
Avg. dist.	7	6.7	6.4	7	6.8	6.4	7.2	6.9	6.5	**4.7**	7.2
Deltas											
TP	736	725	723	709	747	753	705	714	**754**	700	717
FP	17	1	3	13	22	17	44	8	28	**0**	12
FN	32	43	45	59	21	15	63	54	**14**	68	51
TN	1216	1231	1229	1219	1211	1215	1192	1224	1204	**1232**	1220
PREC	.977	.999	.996	.982	.971	.978	.941	.989	.964	**1**	.984
REC	.958	.944	.941	.923	.973	.980	.918	.930	**.982**	.911	.934
F	.968	.971	.968	.952	.972	**.979**	.929	.958	.973	.954	.958
Avg. dist.	4.4	4.1	**4**	4.2	4.3	4.3	4.5	4.1	4.3	4.5	4.9
Total											
Comb. F	.977	.980	.981	.958	.980	**.987**	.943	.963	.983	.966	.966
PDP	92.40	93.50	94.30	85.20	93.60	**95.90**	80.50	87.00	94.60	88.80	89.90

Table 4: Results gathered by each SP detection method on the Sfinge Dataset 1 (1000 fingerprints, profile HQNoPert).

	Template-based SP detection									Poincaré	Liu
Quant.	**C1**	**C2**	**C3**	**C4**	**C5**	**C6**	**C7**	**C8**	**C9**		
Cores											
TP	1295	1299	1312	1256	1305	**1319**	1254	1264	1315	1230	1317
FP	11	9	9	**6**	11	14	26	**6**	20	16	76
FN	37	33	20	76	27	**13**	78	68	17	102	15
TN	659	660	659	**663**	659	654	648	**663**	649	655	594
PREC	.992	.993	.993	**.995**	.992	.989	.980	**.995**	.985	.987	.945
REC	.972	.975	.985	.943	.980	**.990**	.941	.949	.987	.923	.989
F	.982	.984	.989	.968	.986	**.990**	.960	.972	.986	.954	.967
Avg. dist.	7.3	6.9	6.7	7.4	7.1	6.7	7.7	7.2	6.7	**4.9**	7.6
Deltas											
TP	713	705	703	685	720	**727**	670	693	**727**	651	698
FP	73	31	36	44	87	80	105	38	117	29	**18**
FN	44	52	54	72	37	**30**	87	64	**30**	106	59
TN	1172	1213	1209	1202	1159	1164	1151	1208	1132	1218	**1225**
PREC	.907	.958	.951	.940	.892	.901	.865	.948	.861	.957	**.975**
REC	.942	.931	.929	.905	.951	**.960**	.885	.915	**.960**	.860	.922
F	.924	.944	.940	.922	.921	.930	.875	.931	.908	.906	**.948**
Avg. dist.	4.8	4.6	**4.5**	4.9	4.7	4.7	5.2	4.7	4.6	4.8	5.6
Total											
Comb. F	.953	.964	**.964**	.945	.954	.960	.918	.952	.947	.930	.958
PDP	85.60	89.20	**90.00**	82.70	86.00	88.50	74.50	84.50	84.40	79.30	87.20

Table 5: Results gathered by each SP detection method on the Sfinge Dataset 2 (1000 fingerprints, profile Default).

Quant.	Template-based SP detection C1	C2	C3	C4	C5	C6	C7	C8	C9	Poincaré	Liu
Cores											
TP	1140	1141	1167	1080	1148	**1176**	1080	1082	1167	1019	1172
FP	27	20	21	15	30	37	30	**12**	42	26	107
FN	50	49	23	110	42	**14**	110	108	23	171	18
TN	786	792	791	798	784	776	786	**801**	772	790	705
PREC	.977	.983	.982	.986	.975	.969	.973	**.989**	.965	.975	.916
REC	.958	.959	.981	.908	.965	**.988**	.908	.909	.981	.856	.985
F	.967	.971	**.981**	.945	.970	.979	.939	.947	.973	.912	.949
Avg. dist.	7.1	6.6	6.4	7.1	6.8	6.4	7.3	6.9	6.4	**5.1**	7.4
Deltas											
TP	656	651	649	629	663	669	620	633	**670**	612	639
FP	96	55	60	67	114	107	111	61	131	34	**13**
FN	42	47	49	69	35	29	78	65	**28**	86	59
TN	1212	1250	1245	1237	1195	1200	1197	1244	1176	1274	**1290**
PREC	.872	.922	.915	.904	.853	.862	.848	.912	.836	.947	**.980**
REC	.940	.933	.930	.901	.950	.958	.888	.907	**.960**	.877	.915
F	.905	.927	.923	.902	.899	.908	.868	.909	.894	.911	**.947**
Avg. dist.	4.9	4.6	**4.5**	4.8	4.8	4.7	5.3	4.7	4.7	4.8	5.4
Total											
Comb. F	.936	.949	**.952**	.924	.935	.944	.904	.928	.934	.912	.948
PDP	83.10	86.60	**88.50**	77.70	83.10	86.70	72.60	79.30	83.50	74.60	84.70

Table 6: Results gathered by each SP detection method on the Sfinge Dataset 3 (1000 fingerprints, profile VQandPert).

situations occurs with most of the SP detection methods (including Liu's method). Interestingly, the RREF leading to the best results in the TSPD method is not that constructed with the pair of automorphisms C5, indicating that non-linear modelling of dissimilarity can play a role in real applications. Specifically, the best-performing version is that using the pair of automorphisms C3, since it generally outperforms all of the other versions of the TSPD method in terms of Combined F and PDP, the SFinGe Dataset 1 being the sole exception to this fact.

It is worth noting that the TSPD methods have advantages over its counterparts other than pure performance. For example, it holds interesting visualization properties when it comes to error correction, partly derived from the simplicity of the method. Indeed, we have not exploited the potential use of multi-scale templates yet as Liu's method does.

Attending at the results obtained by the RREFs and RSMs, we can state that this extension of the REF and SM concepts considered in Fuzzy Sets theory is appropriate to deal with radial data. Even though radial data may be different from scalar data to some extent, vagueness and imprecision are inherent to both types of data in real applications. Hence, concepts from Fuzzy Sets are also interesting to deal with radial data, as we have shown in this paper. Moreover, the parametrizable construction proposed in Section 5.3 allows us to provide a flexible and configurable model, whose results can be adapted to each application.

6. Conclusions

This work has two main contributions. First, we have adapted the concepts of Restricted Equivalence Function (REF) and Similarity Measure (SM) to radial environments. The resulting operators, namely Restricted Radial Equivalence Function (RREF) and Radial Similarity Measure (RSM), capture the expected behaviour and semantics of the original operators, but at the same time embrace the cyclic nature of radial data. In both cases, we have analysed its properties and proposed construction methods. Second, we have proved the validity of the operators in a complex scenario, such as fingerprint analysis. In order to do so, we have presented a framework for Singular Point (SP) detection based on templates, which requires the use of RSMs at the template matching stage. This framework, namely

Template-based Singular Point Detection (TSPD) method, shows promising results and illustrate the usefulness of RSMs for the comparison of radial data in scenarios in which imprecision and ambiguities occur.

We expect to expand the present work in two different lines of research. As for the theoretical aspects, we aim at adapting to radial data several other operators with special relevance in fuzzy set theory, e.g. aggregation operators or dissimilarity functions. Regarding the TSPD method, we intend to improve it by incorporating notions from multi-scale image processing, as well as by designing self-adapting RREFs which are able to modify their behaviour depending on the characteristics of the fingerprint image and/or the ridge orientation map.

Acknowledgements

The authors gratefully acknowledge the financial support of the Spanish Ministry of Science (project TIN2013-40765-P), the Research Services of Universidad Pública de Navarra, as well as the financial support of the Research Foundation Flanders (FWO project 3G.0838.12.N).

References

[1] B. De Baets, H. De Meyer, On the cycle-transitive comparison of artificially coupled random variables, International Journal of Approximate Reasoning 47 (3) (2008) 306–322.
[2] F. Attneave, Dimensions of similarity, The American Journal of Psychology (1950) 516–556.
[3] I. Bloch, On fuzzy distances and their use in image processing under imprecision, Pattern Recognition 32 (11) (1999) 1873–1895.
[4] Y. Rubner, C. Tomasi, L. J. Guibas, The earth mover's distance as a metric for image retrieval, International Journal of Computer Vision 40 (2) (2000) 99–121.
[5] S. Santini, R. Jain, Similarity measures, IEEE Trans. on Pattern Analysis Machine Intelligence 21 (9) (1999) 871–883.
[6] I. Kramosil, J. Michálek, Fuzzy metrics and statistical metric spaces, Kybernetika 11 (5) (1975) 336–344.
[7] A. Tversky, Measures of similarity, Psychological Review 84 (4) (1977) 327–352.
[8] A. Tversky, I. Gati, Studies of similarity, Cognition and Categorization 1 (1978) 79–98.
[9] M. A. Ruzon, C. Tomasi, Edge, junction, and corner detection using color distributions, IEEE Trans. on Pattern Analysis and Machine Intelligence 23 (11) (2001) 1281–1295.
[10] C. Odet, B. Belaroussi, H. Benoit-Cattin, Scalable discrepancy measures for segmentation evaluation, in: Proc. of the International Conf. on Image Processing, Vol. 1, 2002, pp. 785–788.
[11] L. A. Zadeh, Similarity relations and fuzzy orderings, Information Sciences 3 (2) (1971) 177–200.
[12] B. De Baets, H. De Meyer, H. Naessens, A class of rational cardinality-based similarity measures, Journal of Computational and Applied Mathematics 132 (1) (2001) 51–69.
[13] B. De Baets, H. De Meyer, Transitivity-preserving fuzzification schemes for cardinality-based similarity measures, European Journal of Operational Research 160 (3) (2005) 726–740.
[14] H. Bustince, E. Barrenechea, M. Pagola, Restricted equivalence functions, Fuzzy Sets and Systems 157 (17) (2006) 2333–2346.
[15] F. Zhang, E. R. Hancock, New Riemannian techniques for directional and tensorial image data, Pattern Recognition 43 (4) (2010) 1590–1606.
[16] M. Galar, J. Derrac, D. Peralta, I. Triguero, D. Paternain, C. Lopez-Molina, S. García, J. M. Benítez, M. Pagola, E. Barrenechea, H. Bustince, F. Herrera, A survey of fingerprint classification part I: Taxonomies on feature extraction methods and learning models, Knowledge-Based Systems 81 (2015) 76 – 97.
[17] K. Karu, A. K. Jain, Fingerprint classification, Pattern Recognition 29 (3) (1996) 389–404.
[18] K. Nilsson, J. Bigun, Localization of corresponding points in fingerprints by complex filtering, Pattern Recognition Letters 24 (13) (2003) 2135–2144.
[19] C. I. Watson, C. L. Wilson, NIST Special Database 4, Fingerprint Database, Tech. rep., U.S. National Institute of Standards and Technology (1992).
[20] M. Kawagoe, A. Tojo, Fingerprint pattern classification, Pattern Recognition 17 (3) (1984) 295–303.
[21] M. Liu, Fingerprint classification based on Adaboost learning from singularity features, Pattern Recognition 43 (2010) 1062–1070.
[22] V. Gregori, S. Morillas, A. Sapena, Examples of fuzzy metrics and applications, Fuzzy Sets and Systems 170 (1) (2011) 95–111.
[23] E. Palmeira, B. Bedregal, H. Bustince, A generalization of a characterization theorem of restricted equivalence functions, in: H. Bustince, J. Fernandez, R. Mesiar, T. Calvo (Eds.), Aggregation Functions in Theory and in Practise, Vol. 228 of Advances in Intelligent Systems and Computing, Springer Berlin Heidelberg, 2013, pp. 453–464.
[24] A. Jurio, M. Pagola, D. Paternain, C. Lopez-Molina, P. Melo-Pinto, Interval-valued restricted equivalence functions applied on clustering techniques, in: Proc. of the IFSA-EUSFLAT, 2009, pp. 831–836.
[25] L. Xuecheng, Entropy, distance measure and similarity measure of fuzzy sets and their relations, Fuzzy Sets and Systems 52 (3) (1992) 305–318.
[26] G. Beliakov, A. Pradera, T. Calvo, Aggregation Functions: A Guide for Practitioners, Vol. 221 of Studies in Fuzziness and Soft Computing, Springer, 2007.
[27] N. I. Fisher, Statistical Analysis of Circular Data, Cambridge University Press, 1993.
[28] E. Batschelet, Circular statistics in biology, Academic Press, 1981.
[29] J. C. Davis, R. J. Sampson, Statistics and data analysis in geology, Vol. 3, Wiley New York, 2002.
[30] K. V. Mardia, P. E. Jupp, Directional statistics, Wiley, 2000.

[31] D. Peralta, M. Galar, I. Triguero, D. Paternain, S. García, E. Barrenechea, J. M. Benítez, H. Bustince, F. Herrera, A survey on fingerprint minutiae-based local matching for verification and identification: Taxonomy and experimental evaluation, Information Sciences 315 (2015) 67–87.
[32] L. Hong, Y. Wan, A. Jain, Fingerprint image enhancement: Algorithm and performance evaluation, IEEE Trans. on Pattern Analysis and Machine Intelligence 20 (8) (1998) 777–789.
[33] D. Peralta, M. Galar, I. Triguero, O. Miguel-Hurtado, J. M. Benitez, F. Herrera, Minutiae filtering to improve both efficacy and efficiency of fingerprint matching algorithms, Engineering Applications of Artificial Intelligence 32 (2014) 37–53.
[34] X. Jiang, W.-Y. Yau, Fingerprint minutiae matching based on the local and global structures, in: Proc. of the International Conf. on Pattern Recognition, Vol. 2, 2000, pp. 1038–1041.
[35] X. Chen, J. Tian, X. Yang, A new algorithm for distorted fingerprints matching based on normalized fuzzy similarity measure, IEEE Trans. on Image Processing 15 (3) (2006) 767–776.
[36] D. Peralta, I. Triguero, S. García, F. Herrera, J. M. Benitez, Dpd-dff: A dual phase distributed scheme with double fingerprint fusion for fast and accurate identification in large databases, Information Fusion 32, Part A (2016) 40 – 51.
[37] M. Galar, J. Derrac, D. Peralta, I. Triguero, D. Paternain, C. Lopez-Molina, S. García, J. M. Benítez, M. Pagola, E. Barrenechea, H. Bustince, F. Herrera, A survey of fingerprint classification part II: Experimental analysis and ensemble proposal, Knowledge-Based Systems 81 (2015) 98 – 116.
[38] K. Cao, L. Pang, J. Liang, J. Tian, Fingerprint classification by a hierarchical classifier, Pattern Recognition 46 (12) (2013) 3186–3197.
[39] D. Maltoni, D. Maio, A. K. Jain, S. Prabhakar, Handbook of fingerprint recognition, Springer-Verlag, 2009.
[40] R. Cappelli, D. Maio, D. Maltoni, SFinGe: An approach to synthetic fingerprint generation, in: International Conf. on Control, Automation, Robotics and Vision, 2004.
[41] Q. Zhang, H. Yan, Fingerprint classification based on extraction and analysis of singularities and pseudo ridges, Pattern Recognition 37 (11) (2004) 2233–2243.
[42] J.-H. Hong, J.-K. Min, U.-K. Cho, S.-B. Cho, C. H. Leung, Fingerprint classification using one-vs-all support vector machines dynamically ordered with naive bayes classifiers, Pattern Recognition 41 (2008) 662–671.
[43] J. Li, W.-Y. Yau, H. Wang, Combining singular points and orientation image information for fingerprint classification, Pattern Recognition 41 (1) (2008) 353–366.
[44] A. K. Jain, S. Minut, Hierarchical kernel fitting for fingerprint classification and alignment, in: Proc. of the International Conf. on Pattern Recognition, 2002, pp. 469–473.
[45] A. M. Bazen, S. H. Gerez, Systematic methods for the computation of the directional fields and singular points of fingerprints, IEEE Transactions on Pattern Analysis and Machine Intelligence 24 (7) (2002) 905–919.
[46] Y. Mei, R. Hou, J. Wang, An improved method for fingerprints' singular points detection based on orientation field partition, International Journal of Signal Processing, Image Processing and Pattern Recognition 6 (1) (2013) 225–234.
[47] F. Turroni, D. Maltoni, R. Cappelli, D. Maio, Improving fingerprint orientation extraction, IEEE Trans. on Information Forensics and Security 6 (3) (2011) 1002–1013.
[48] M. Kass, A. Witkin, Analyzing oriented patterns, Computer Vision Graphics and Image Processing 37 (3) (1987) 362–385.
[49] S. Chaudhuri, S. Chatterjee, N. Katz, M. Nelson, M. Goldbaum, Detection of blood vessels in retinal images using two-dimensional matched filters, IEEE Trans. on Medical Imaging 8 (3) (1989) 263–269.
[50] R. Poli, G. Valli, An algorithm for real-time vessel enhancement and detection, Computer Methods and Programs in Biomedicine 52 (1) (1997) 1–22.
[51] M. H. Hueckel, An operator which locates edges in digitized pictures, Journal of the ACM 18 (1) (1971) 113–125.
[52] Y. Li, X. lin Qi, Y. jiu Wang, Eye detection by using fuzzy template matching and feature-parameter-based judgement, Pattern Recognition Letters 22 (10) (2001) 1111–1124.
[53] J. Serra, Introduction to mathematical morphology, Computer Vision, Graphics, and Image Processing 35 (3) (1986) 283–305.
[54] C. Marco-Detchart, J. Cerron, L. De Miguel, C. Lopez-Molina, H. Bustince, M. Galar, Singular point location for NIST-4 database (2015). URL `https://giara.unavarra.es/datasets/solNIST4.zip`
[55] D. Maio, D. Maltoni, R. Cappelli, J. L. Wayman, A. K. Jain, FVC2000: Fingerprint verification competition, IEEE Trans. on Pattern Analysis Machine Intelligence 24 (3) (2002) 402–412.
[56] D. Maio, D. Maltoni, R. Cappelli, J. L. Wayman, A. K. Jain, FVC2002: Second fingerprint verification competition, in: Proc. of the International Conf. on Pattern Recognition, 2002, pp. 811–814.
[57] D. Maio, D. Maltoni, R. Cappelli, J. L. Wayman, A. K. Jain, FVC2004: Third fingerprint verification competition, in: Proc. of the International Conf. on Biometric Authentication, 2004, pp. 1–7.
[58] R. Cappelli, M. Ferrara, A. Franco, D. Maltoni, Fingerprint Verification Competition 2006, Biometric Technology Today 15 (7-8) (2007) 7–9.
[59] B. Dorizzi, R. Cappelli, M. Ferrara, D. Maio, D. Maltoni, N. Houmani, S. Garcia-Salicetti, A. Mayoue, Fingerprint and on-line signature verification competitions at ICB 2009, in: M. Tistarelli, M. Nixon (Eds.), Advances in Biometrics, Vol. 5558 of Lecture Notes in Computer Science, Springer Berlin Heidelberg, 2009, pp. 725–732.
[60] I. Sobel, G. Feldman, A 3x3 isotropic gradient operator for image processing, presented at a talk at the Stanford Artificial Intelligence Project (1968).
[61] J. M. S. Prewitt, Object enhancement and extraction, Picture Processing and Psychopictorics, Academic Press, 1970, pp. 75–149.
[62] P. L. Rosin, Edges: saliency measures and automatic thresholding, Machine Vision and Applications 9 (1997) 139–159.
[63] X. Liu, Y. Yu, B. Liu, Z. Li, Bowstring-based dual-threshold computation method for adaptive Canny edge detector, in: Proc. of the International Conf. of Image and Vision Computing New Zealand, 2013, pp. 13–18.
[64] H. O. Nyongesa, S. Al-Khayatt, S. M. Mohamed, M. Mahmoud, Fast robust fingerprint feature extraction and classification, Journal of Intelligent and Robotic Systems 40 (1) (2004) 103–112.